

NASA TECHNICAL NOTE



NASA TN D-5744

ext. 12
c. 1

NASA TN D-5744



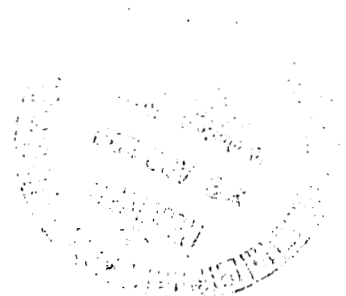
LOAN COPY: RETURN TO
AFWL (WLOL)
KIRTLAND AFB, N MEX

DESIGN STUDY OF SHAFT FACE SEAL WITH SELF-ACTING LIFT AUGMENTATION

I - Self-Acting Pad Geometry

*by John Zuk, Lawrence P. Ludwig,
and Robert L. Johnson*

*Lewis Research Center
Cleveland, Ohio*





0131519

1. Report No. NASA TN D-5744	2. Government Accession No.	3. Recipient's Catalog No.	
4. Title and Subtitle DESIGN STUDY OF SHAFT FACE SEAL WITH SELF-ACTING LIFT AUGMENTATION I - SELF-ACTING PAD GEOMETRY		5. Report Date April 1970	
		6. Performing Organization Code	
7. Author(s) John Zuk, Lawrence P. Ludwig, and Robert L. Johnson		8. Performing Organization Report No. E-5453	
9. Performing Organization Name and Address Lewis Research Center National Aeronautics and Space Administration		10. Work Unit No. 126-15	
		11. Contract or Grant No.	
12. Sponsoring Agency Name and Address National Aeronautics and Space Administration Washington, D.C. 20546		13. Type of Report and Period Covered Technical Note	
		14. Sponsoring Agency Code	
15. Supplementary Notes			
16. Abstract The load capacity of several self-acting pad geometries was calculated for various pad recess depths, film thicknesses, and angular deformations. The study revealed that the self-acting pad geometry had a high gas film stiffness. This high gas film stiffness is inherently suited for seal operation since the lift force drops off rapidly if the seal tends to open; hence, the seal will not remain open at a large film thickness, which would allow high leakage. Also, this high gas film stiffness forces the seal nosepiece to dynamically track the face runout of the rotor. The load capacity calculations showed that the self-acting pad geometry can accommodate practical face deformations.			
17. Key Words (Suggested by Author(s)) Face seal Self-acting geometry Gas bearings Seal Gas film seal		18. Distribution Statement Unclassified - unlimited	
19. Security Classif. (of this report) Unclassified	20. Security Classif. (of this page) Unclassified	21. No. of Pages 39	22. Price* \$3.00

*For sale by the Clearinghouse for Federal Scientific and Technical Information
Springfield, Virginia 22151



DESIGN STUDY OF SHAFT FACE SEAL WITH SELF-ACTING LIFT AUGMENTATION

I - SELF-ACTING PAD GEOMETRY

by John Zuk, Lawrence P. Ludwig, and Robert L. Johnson

Lewis Research Center

SUMMARY

A parametric design study was made on a face seal with a self-acting pad geometry having a 6.5-inch (16.5-cm) nominal diameter. The load carrying capacity of the self-acting pad geometry was calculated for various pad recess depths, film thicknesses, angular deformations, and self-acting pad geometries. The self-acting pad geometries had a characteristically steep gradient (high gas film stiffness) of lift force against film thickness. This high gas film stiffness is advantageous in that the lift force drops off rapidly if the seal tends to open; hence, the closing force increases rapidly. If the seal tends to close, the opposite effect occurs. A small operating gas film thickness, therefore, is maintained, and the high gas film stiffness forces the seal nosepiece to dynamically track the runout motion of the seal face. The shallower recess depths produce steeper gradients of lift force against film thickness, but for wear considerations, a deeper recess depth of 0.001 inch (0.003 cm) was selected. Angular deformation of the sealing face did not have a significant effect on the load carrying capacity of the self-acting pads.

INTRODUCTION

Shaft seal systems in advanced turbine engines will be operated at speeds, temperatures, and pressures higher than those currently used. Conventional face seals presently in use in some gas turbine engines are limited to a sliding velocity of about 350 feet per second (107 m/sec), a gas temperature of 800^o F (700 K), and a pressure of 125 psi (86.1 N/cm²) (ref. 1). Advanced engines will require seals to operate at 500 feet per second (152 m/sec) (ref. 2), and pressures to 500 psi (344 N/cm²) (ref. 3) are anticipated. Face seals for these high speeds and pressures must operate with positive sealing face separation (no rubbing contact) in order to achieve long life and reliability. Some

conventional face seals used in current engines apparently operate with positive face separation under steady-state conditions, but this positive face separation is not assured by the design procedure. Extension of the speed, pressure, and temperature limitations of a conventional face seal will be minimal unless the design ensures the small but vital positive sealing face separation.

A direct approach to obtaining positive sealing face separation is found in the hydrostatic and self-acting seal designs under investigation in the studies reported in references 4 and 5. The self-acting seal design, which has a low leakage potential (ref. 5), is a conventional face seal with a self-acting pad geometry (step-type gas-lubricated bearings) for lift augmentation (see fig. 1). It should be noted that, in the conventional face seal, divergent sealing faces lead to loss of seal opening force; hence, rubbing contact can occur (ref. 5). However, as pointed out in reference 5, the step-type gas bearing added to a conventional face seal acts to maintain sealing surface separation even though adverse sealing face deformation occurs. The feasibility of the self-acting face seal has been demonstrated in several NASA sponsored programs (ref. 5). Recent data show satisfactory performance to a speed of 400 feet per second (122 m/sec), a pressure of 250 psi (172 N/cm²), and a sealed gas temperature of 1000^o F (810 K).

The design of the self-acting geometry is vital to seal dynamic performance. The self-acting geometry must provide

- (1) Sufficient lift force to separate the surfaces at less than idle speed
- (2) Sufficient gas film stiffness to make the nosepiece dynamically track the axial motions of the seal seat face

A necessary step in optimization of lift augmentation in a face seal is a parametric study of the self-acting geometry. Thus, the objectives of the present work are to determine for a seal of practical interest

- (1) A practical pad recess depth for the self-acting geometry
- (2) The effect of the number of self-acting pads
- (3) The effect of thermal deformation on load capacity

The parametric study was made on a face seal with a self-acting lift geometry having a 6.5-inch (16.5-cm) nominal diameter. Sealed gas pressures of 65, 215, and 315 psia (45, 148, and 217 N/cm² abs) were considered. The load carrying capacity of the self-acting geometry was calculated for various pad recess depths, film thicknesses, angular deformations, and for a number of self-acting pads.

DESCRIPTION OF FACE SEAL WITH SELF-ACTING GEOMETRY

Figure 1 shows a face-type seal with a self-acting pad geometry that consists of a series of shallow recesses arranged circumferentially around the seal under the sealing

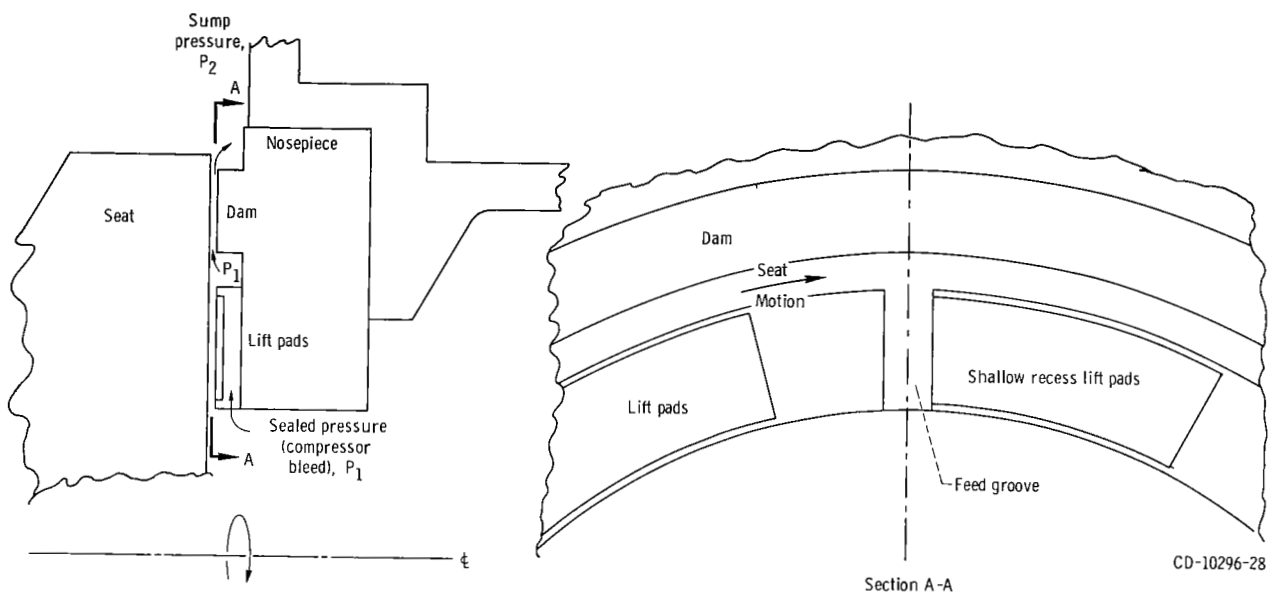
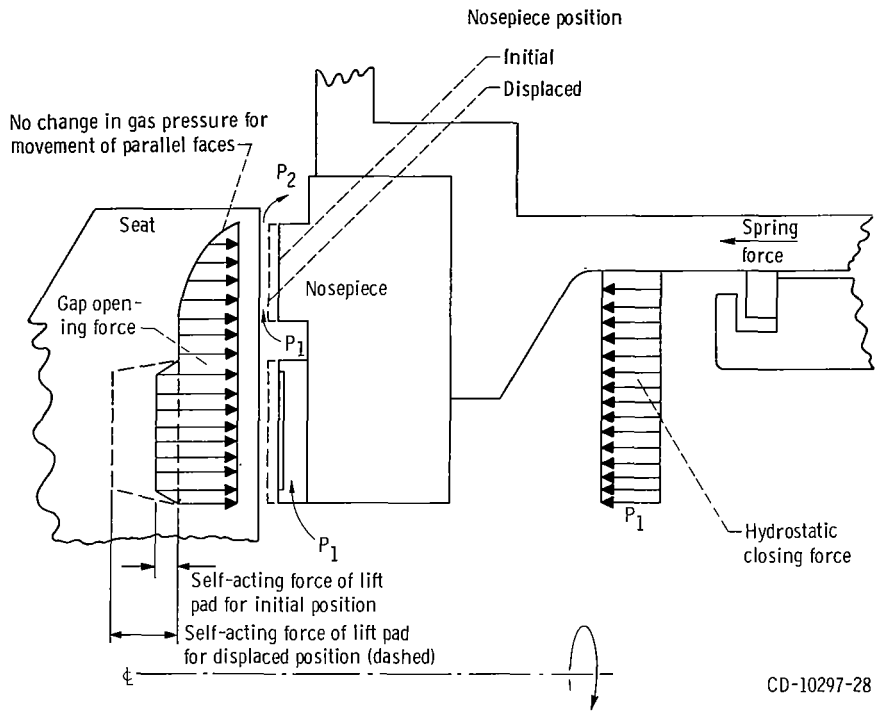
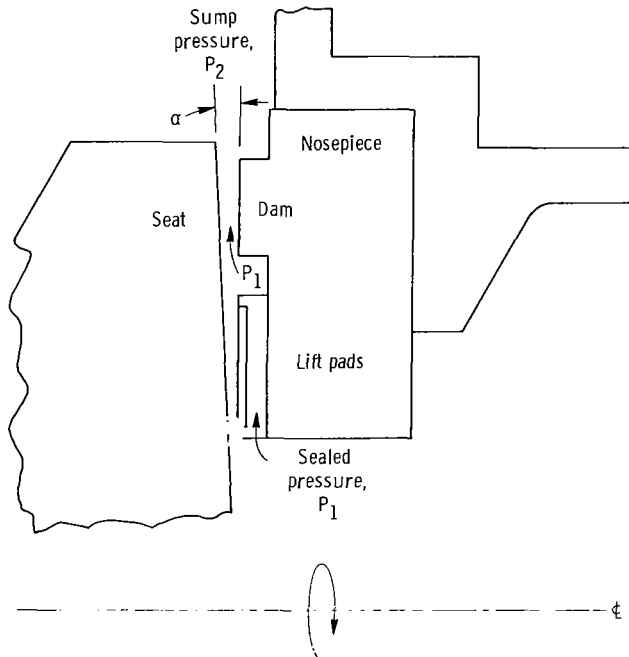


Figure 1. - Face seal with self-acting lift pads.

dam. It should be noted that the lift geometries are bounded at the inside and outside diameters by the sealed pressure P_1 . This is accomplished by feed slots that connect the annular groove directly under the sealing dam with the sealed pressure in the cavity. The effect of the self-acting geometry on face seal operation is illustrated in figure 2, which shows parallel sealing faces operating without rubbing contact because of a balance between the closing force and the opening force, that is, the self-acting lift force plus the pressure acting between the sealing faces. If the seal tends to close, the gas bearing force increases to prevent rubbing contact; thus, a condition of no rubbing contact can prevail except at startup and shutdown.



(a) Mechanical, pneumatic, and self-acting forces on seal nosepiece.



(b) Seal with exaggerated face deformation (coning or dishing).

Figure 2. - Self-acting face seal.

RESULTS AND DISCUSSION

Design Points

For the purpose of analysis, three design points were selected as representative of operating conditions in the advanced gas turbine (see table I).

Model of Self-Acting Lift Geometry

A single self-acting pad (shrouded step-type), which served as the mathematical model, is shown in figure 3. The radial width b of all pads was 0.20 inch (0.507 cm), and the length c was determined by the number of pads arranged circumferentially under the sealing dam. Because of the large radius-to-pad width ratio r/b , the curvature was neglected in the mathematical model. Thus, the pad boundaries conform to a Cartesian coordinate system. The feed-groove width f was held constant for all pads. The recess length-to-land length ratio R/L was varied between 0.4 and 1.8. Also, the effect on load capacity of the ratio of recess depth to film thickness Δ/h_m was determined over the range of $(\Delta + h_m)/h_m = 0.52$ to 6.0. (All symbols are defined in appendix A.) Calculations of load capacity were made for the parallel film face and for the case with a

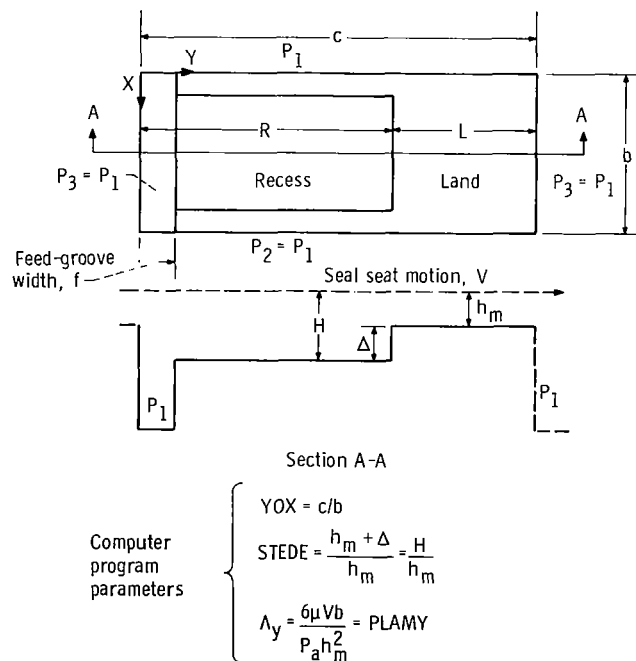


Figure 3. - Model of single self-acting pad (shrouded Rayleigh step type).

2-milliradian angular deformation. This angular deformation was chosen as a practical case that might occur as the result of thermal gradients. Figure 4 shows the actual dimensions of one of the pad designs.

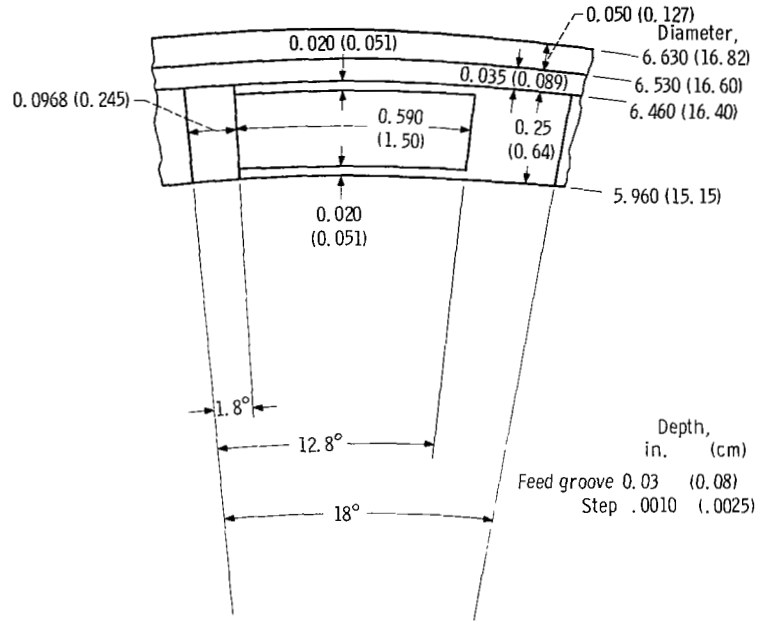


Figure 4. - Details of sealing dam and self-acting pad geometry. All dimensions are in inches (cm).

The computer program listing in reference 5, which is valid for a shrouded lift pad, is used for this study. This computer program has been modified (as shown in appendix B) so that it can be used on the Lewis Research Center computer, and the input has been modified for NAMELIST to facilitate parametric design studies. The program solves the complete two-dimensional compressible flow Reynolds lubrication equation written in the P^2 form

$$\frac{\partial}{\partial X} \left(\frac{H^3}{2} \frac{\partial P^2}{\partial X} \right) + \frac{\partial}{\partial Y} \left(\frac{H^3}{2} \frac{\partial P^2}{\partial Y} \right) = \Lambda_x \frac{\partial(PH)}{\partial X} + \Lambda_y \frac{\partial(PH)}{\partial Y}$$

where

$$\Lambda_x = \frac{6\mu Ub}{P_a h_m^2} \quad \Lambda_y = \frac{6\mu Vb}{P_a h_m^2}$$

The formulation of this analysis is given in reference 6. For details of the solution of the foregoing equation, see appendix B in reference 7. A discussion of the use of the program for a nonparallel film is given in appendix A of reference 5. The following assumptions or restrictions apply in the present analysis:

(1) The fluid is Newtonian and viscous. A laminar flow regime is assumed. It should be noted that it is possible for the seal assembly to be operated in the transition or slip flow regime for clearances less than 0.0001 inch (0.0003 cm), and the analysis is not valid in this slip regime.

(2) The bulk modulus, $3\lambda + 2\mu = 0$, is Stokes idealization and is valid since local shocks are not present and the flow is analyzed for the continuum flow regimes.

(3) The body forces are negligible.

(4) The flow is laminar for a maximum film thickness of 0.001 inch (0.003 cm). The maximum Reynolds number is 658, which is considerably less than the minimum transition rotational Reynolds number of about 1900.

(5) The modified or reduced pressure flow Reynolds number is much less than 1. For example, at design point 3 in table I, the modified Reynolds number is in the range of 0.023. Thus, the Reynolds equation should be valid for the model of the self-acting lift pad.

TABLE I. - DESIGN POINTS

	Design Point		
	1	2	3
Velocity, V, ft/sec (m/sec)	200 (61)	500 (153)	450 (137)
Sealed gas pressure, P ₁ , psia (N/cm ² abs)	65 (45)	215 (148)	315 (217)
Sealed gas temperature, T ₁ , °F (K)	100 (311)	800 (700)	1300 (977)
Sump pressure, P ₂ , psia (N/cm ² abs)	15 (10.3)	15 (10.3)	15 (10.3)
Viscosity, μ, (lb)(sec)/in. ² (N)(sec)/cm ²)	2.75×10 ⁻⁹ (19×10 ⁻¹⁰)	4.87×10 ⁻⁹ (3.36×10 ⁻¹⁰)	6.00×10 ⁻⁹ (4.14×10 ⁻¹⁰)
Operating condition	Descent	Takeoff and climb	Cruise

The compressibility number Λ_y was calculated for each of the three design points (see table I) at various film thicknesses (see table II) by using the following relations:

Design point 1:

$$\Lambda_y = \frac{15.2 \times 10^{-8}}{h_m^2}$$

Design point 2:

$$\Lambda_y = \frac{20.4 \times 10^{-8}}{h_m^2}$$

Design point 3:

$$\Lambda_y = \frac{15.4 \times 10^{-8}}{h_m^2}$$

Effect of Number of Self-Acting Lift Pads

The load capacity of the self-acting pads as a function of the number of pads is shown in figure 5. As the number of pads increases, the circumferential length of each pad

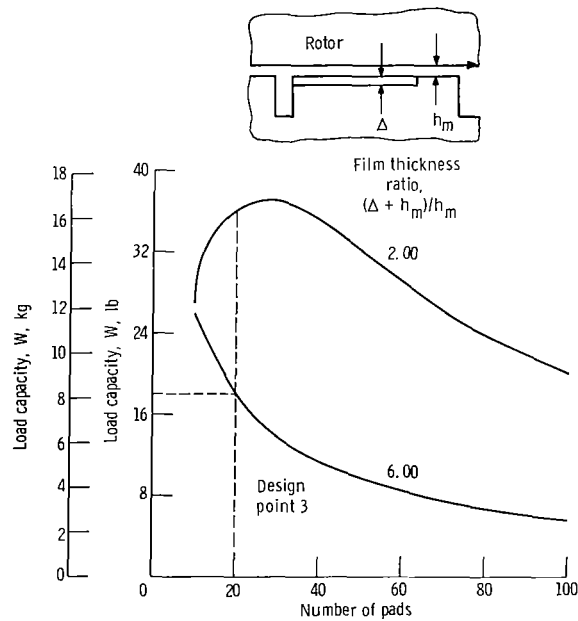


Figure 5. - Load capacity of shrouded self-acting lift pads as function of number of pads. Sealed pressure, 315 psia (217 N/cm² abs); sealed gas temperature, 1300° F (977 K); sliding velocity, 450 feet per second (137 m/sec).

necessarily decreases in order to fit the available region under the sealing dam. The calculations were made at design point 3, which has a pressure differential of 300 psi (206 N/cm²) and a sealed gas temperature of 1300° F (977 K). The sliding velocity was 450 feet per second (137 m/sec). At a film thickness ratio of $(\Delta + h_m)/h_m = 2$, which is a practical ratio for a large operating film thickness, an optimum is indicated at 28 pads. However, at a film thickness ratio of $(\Delta + h_m)/h_m = 6$, which is a practical ratio for a small operating thickness, no optimum is indicated and the load capacity increases as the number of pads decreases. Since the seal is expected to operate at various film thicknesses, a compromise in the number of pads must be sought, and the number selected was 20.

Effect of Recess Length-to-Land Length Ratio

The load capacity as a function of recess length-to-land length ratio R/L for symmetric and asymmetric designs is shown in figure 6. The calculation was made for design point 3 of table I with the film thickness ratio of $(\Delta + h_m)/h_m = 6$. A symmetric design has a slightly greater load capacity than an asymmetric design, and the curve trend suggests that a recessed land length ratio R/L of 1.8 or greater will provide near optimum capacity. Because of wear considerations, it is desirable to have the land length as

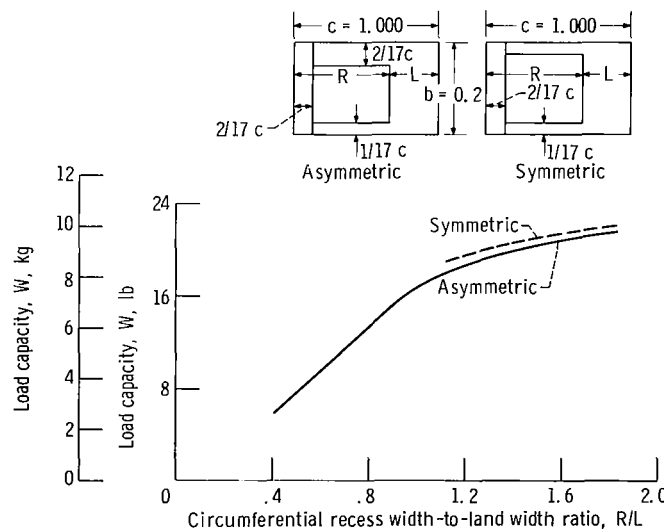


Figure 6. - Load capacity of shrouded self-acting lift pads as function of recess length-to-land length ratio. Sealed pressure, 315 psia (217 N/cm² abs); sealed gas temperature, 1300° F (977 K); sliding velocity, 450 feet per second (137 m/sec); number of pads, 20; film thickness ratio, 6; compressibility number in circumferential direction, 1.78.

long as practical; therefore, a recess-to-land length ratio of 1.4 was selected as a compromise between wear and load capacity considerations.

Effect of Recess Depth-to-Film Thickness Ratio

The load capacity as a function of film thickness ratio $(\Delta + h_m)/h_m$ is shown in figure 7. The optimum film thickness ratio is near $(\Delta + h_m)/h_m = 2$. However, under dy-

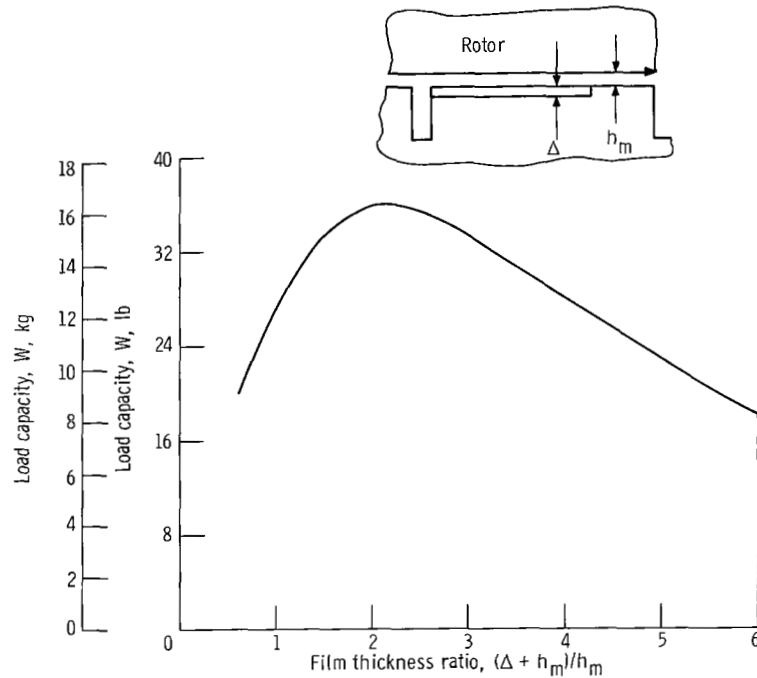


Figure 7. - Load capacity of shrouded self-acting lift pads as function of film thickness ratio. Sealed pressure, 315 psia (217 N/cm² abs); sealed gas temperature, 1300° F (977 K); sliding velocity, 450 feet per second (137 m/sec); number of pads, 20.

amic operation, the film thickness is expected to vary because of the inherent runout of the seal seat face. Thus, in operation, a range of film thickness ratios is expected. Because of leakage considerations, the film thickness of 0.0004 inch (0.0010 cm) is a practical average operating condition; and for this case, the recess depth would be 0.0004 inch (0.0010 cm) to achieve the optimum value of $(\Delta + h_m)/h_m = 2$. However, in order to provide increased wear capability, a recess depth of 0.001 inch (0.00254 cm) was selected. Thus, for a film thickness of 0.0004 inch (0.0010 cm), the film thickness ratio is $(\Delta + h_m)/h_m = 3.5$.

Load Capacity as Function of Film Thickness

The load capacity for the three design points listed in table I is shown in figure 8.

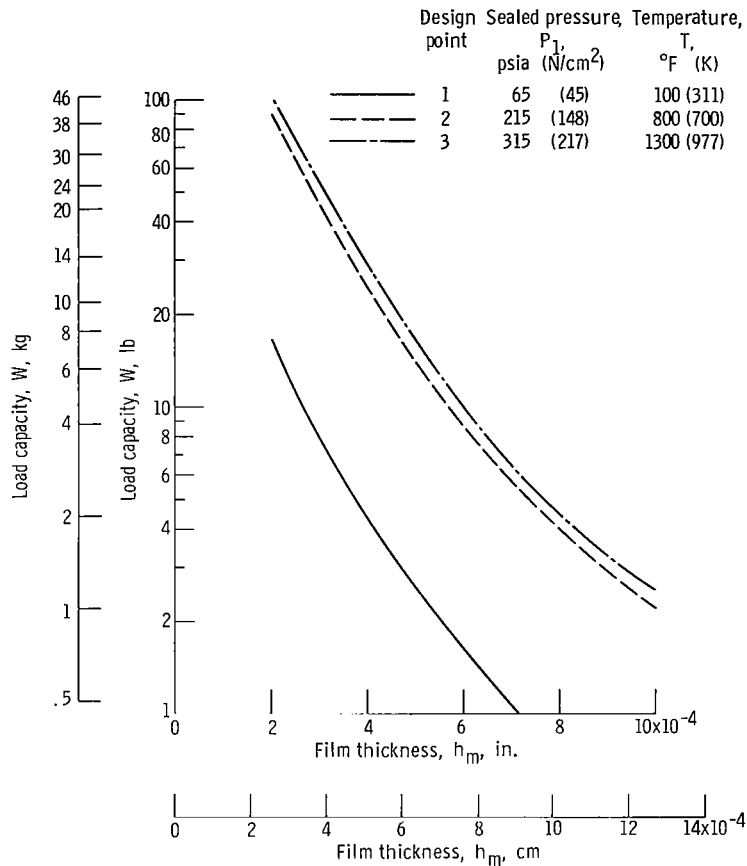


Figure 8. - Load capacity of shrouded self-acting lift pads as function of film thickness. Number of pads, 20; recess length to-land length ratio, 1.4.

The calculations are for 20 pads and a recess depth of 0.001 inch (0.003 cm). The curves reveal a high film stiffness that is advantageous for seal operations; that is, at low film thicknesses, a high lift force is produced to prevent rubbing contact and at high film thicknesses, which would have high leakage, only a low lift force is produced. Thus, if the seal opens, the pad lift force drops off sharply, and the closing force acts to return the nose to the equilibrium condition.

Effect of Face Angular Deformation

The effect of face angular deformation on load capacity is shown in figure 9. A deformation of 2 milliradians was selected as a practical value that might occur as a result of axial thermal gradients in the seal faces. This angular deformation results in a loss in load capacity. For example, figure 9 shows a 27-pound (12-kg) load capacity for parallel faces and a 21-pound (9.5-kg) load capacity for faces with a mean film thickness of 0.0004 inch (0.0010 cm) and a 2-milliradian deformation. This loss in load capacity is not excessive and indicates that the self-acting geometry can accommodate some face

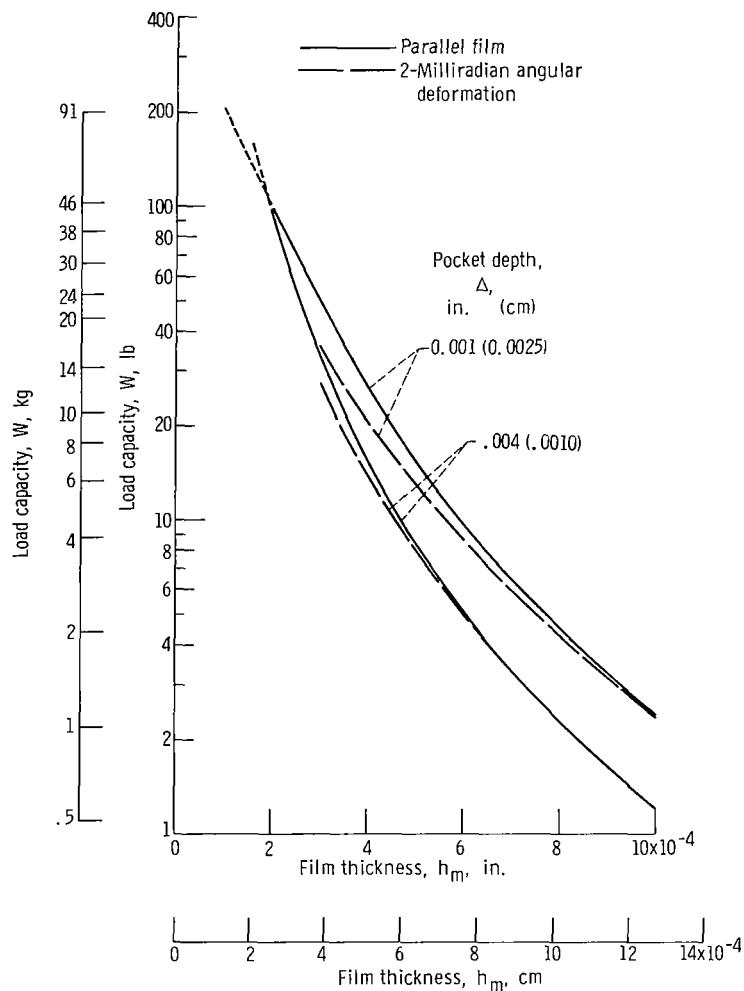


Figure 9. - Load capacity of self-acting geometry as function of angular deformation. Sealed pressure, 315 psia (217 N/cm² abs); sealed gas temperature, 1300° F (977 K); sliding velocity 400 feet per second (122 m/sec); number of pads, 20; recess length-to-land length ratio, 1.4; recess depths, 0.0010 inch (0.0025 cm) and 0.0004 inch (0.0010 cm).

deformation. (See ref. 5 for discussion of techniques in minimizing deformations in seals.)

Effect of Recess Depth on Film Stiffness

The 0.001-inch (0.003-cm) recess depth was selected as a practical value because a compromise between wear and load capacity was necessary. A comparison of the 0.001-inch (0.003-cm) depth with the 0.0004-inch (0.0010-cm) depth demonstrates the penalty paid for the compromise. Figure 10 shows load capacity as a function of film thickness for each of the two recess depths. The 0.001-inch (0.003-cm) recess depth has a greater load capacity except at very small film thicknesses, that is, at 0.0002 inch (0.0005 cm) and below. The important point is that the shallow recess has a higher film stiffness

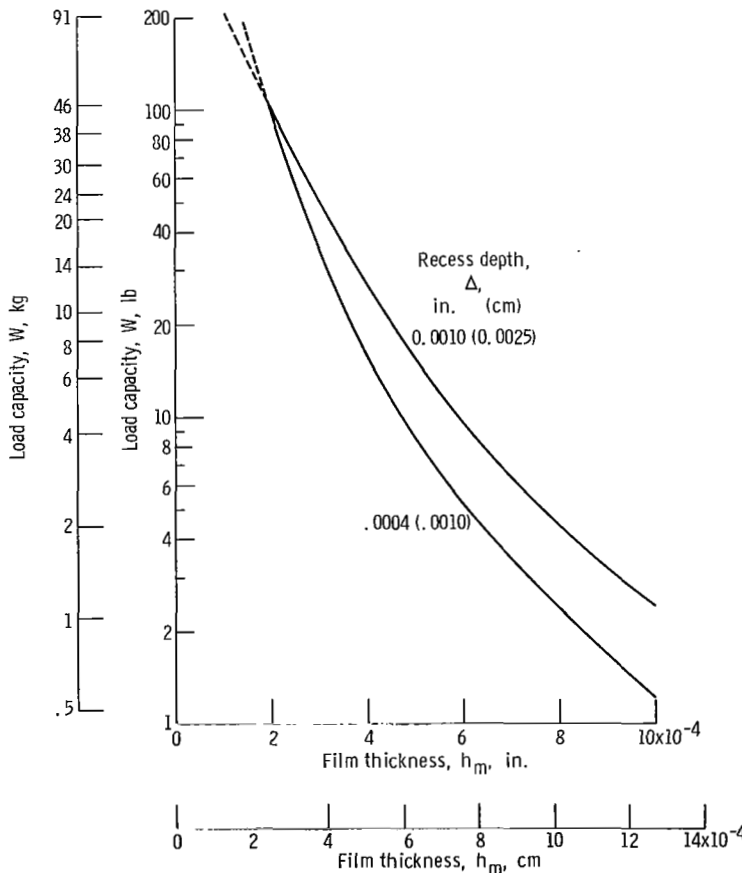


Figure 10. - Effect of recess depth on load capacity of self-acting lift pads. Sealed pressure, 315 psia (217 N/cm² abs); sealed gas temperature, 1300° F (977 K); sliding velocity, 450 feet per second (137 m/sec); number of pads, 20; recess length-to-land length ratio, 1.4.

(curve of steeper load against film height), and this higher film stiffness is desirable in seal operation; that is, if the seal tends to open, the self-acting force drops off rapidly and, hence, the closing force increases rapidly. If the seal tends to close, the opposite effect occurs.

SUMMARY OF RESULTS

A parametric study was made on a face seal with a self-acting lift geometry having a 6.5-inch (16.5-cm) nominal diameter. Sealed gas pressures of 65, 215, and 315 psia (45, 148, and 217 N/cm² abs) were considered. The load carrying capacity of the self-acting geometry was calculated for various recess depths, film thicknesses, angular deformations, and numbers of self-acting pads. A self-acting geometry was placed on a high-pressure side of the seal dam inside diameter. The analysis yielded the following results:

1. The characteristic steep gradient of lift force against gap height of the self-acting geometry was responsible for maintaining the small sealing gap height necessary for low leakage. That is, if the seal tends to open, the lift force drops off rapidly; hence, the closing force increases rapidly. If the seal tends to close, the opposite effect occurs. Thus, the self-acting geometry provides a high gas film stiffness, which is necessary if the nosepiece is to track dynamically the face runout of the seal seat.

2. The gradient of self-acting lift force against film thickness was affected by the recess pad depth; the shallower recesses produced a steeper gradient.

3. For faces with angular deformation (e. g., due to thermal gradients), the self-acting lift force was less than that for parallel faces. Calculations for practical values of angular deformation indicated that the self-acting geometry produces a useful load.

4. The self-acting pad geometry selected was a compromise between wear and load capacity considerations; that is, the recess depth selected was deeper than the optimum, and the recess length-to-land length ratio was smaller than the optimum.

Lewis Research Center,
National Aeronautics and Space Administration,
Cleveland, Ohio, January 7, 1970,
126-15.

APPENDIX A

SYMBOLS

A	pad area, in. ² ; cm ²
b	self-acting pad radial width, in.; cm
c	self-acting pad circumferential length, in.; cm
f	feed-groove circumferential length, in.; cm
H	recess depth plus film thickness, in.; cm
h	film thickness, in.; cm
L	land circumferential length, in.; cm
P	static pressure, psi; N/cm ²
R	recess circumferential length, in.; cm
r	radius, in.; cm
T	temperature, °F; K
U	moving seal seat radial surface speed, ft/sec; m/sec
V	moving seal seat circumferential surface speed, ft/sec; m/sec
W	load capacity, lb; kg
X	radial coordinate direction
Y	circumferential coordinate direction
α	relative inclination angle of surfaces, mrad
Δ	recess or pocket depth, in.; cm
Λ_x	compressibility number in radial direction, $6\mu Uc/P_a h_m^2$
Λ_y	compressibility number in circumferential direction, $6\mu Vb/P_a h_m^2$
λ	second viscosity coefficient or coefficient of bulk viscosity
μ	absolute or dynamic viscosity, (lb)(sec)/in. ² ; (N)(sec)/cm ²

Subscripts:

a	ambient conditions
m	mean
1	sealed conditions
2	sump conditions

APPENDIX B

COMPUTER PROGRAM FOR SHROUDED SELF-ACTING LIFT PAD

Input Instructions

The computer program is composed of the main program and five subroutines. The main program reads the input, performs the major portion of the calculations, calls on the subroutines, and writes the output. The five subroutines are titled SUM, HFUN, HXFUN, HYFUN, and MATINV.

SUM is the Simpson's rule integration scheme for odd and even mesh points.

HFUN describes the shape of film thickness.

HXFUN describes the derivative of film thickness in X-direction.

HYFUN describes the derivative of film thickness in Y-direction.

MATINV inverts the necessary matrix required by the columnwise influence coefficient method.

The program is coded in FORTRAN IV, version 13, and is run on an IBM 7044-7094 direct couple system with 32K core storage.

Each set of input data requires three major input cards. In addition, the first set requires the seal geometry cards. All input statements are in the NAMELIST form, a feature of FORTRAN IV, version 13. The following is a list of the data cards for a sample problem:

(1) Pad Number Control Card

Item Number (3 items)

(a) NPAD-Control number specifying number of pads to be used

1 - Single pad

2 - Twin pad, extra card (1b) is needed

3 - Twin pad, NPD = TRUE, extra card (1a) is needed

- Triple pad, NPD = FALSE, extra cards (1a and 1b) are needed

(b) INP-Control for input to be continued or terminated

0 - Input set to be continued

1 - Input set to be terminated

(c) NDPP-Control for printout W/A ($P_2 - P_1$)

0 - W/A ($P_2 - P_1$) will be printed out besides W/A P_1

1 - Only W/A P_1 printed out as the load parameter

(1a) Second Pad Geometry Card

Item Number (6 items)

1 - IA, number of mesh points to first step in X-direction for second pad

2 - JA, number of mesh points to first step in Y-direction for second pad

- 3 - IAA, number of mesh points to second step in X-direction for second pad
- 4 - JAA, number of mesh points to second step in Y-direction for second pad
- 5 - STEDA, ratio of step depth to film thickness for second pad
- 6 - NPD = .TRUE. for twin pad
= .FALSE. for triple pad, additional card (1b) is required

(1b) Second or Third Pad Geometry Card

This card is required when NPAD = 2 or NPAD = 3 and NPD = FALSE, and it describes the second or third pad geometry, respectively.

Item Number (5 items)

- 1 - IB, number of mesh points to first step in X-direction for second or third pad
- 2 - JB, number of mesh points to first step in Y-direction for second or third pad
- 3 - IBB, number of mesh points to second step in X-direction for second or third pad
- 4 - JBB, number of mesh points to second step in Y-direction for second or third pad
- 5 - STEDB, ratio of step depth to film thickness for second or third pad

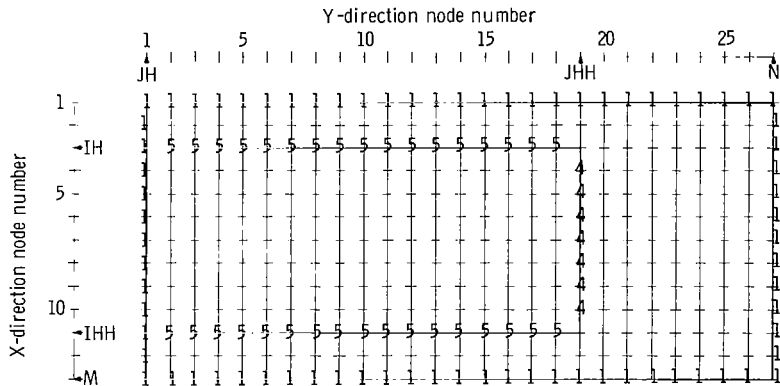


Figure 11. - Sample mesh-point layout. (All nodal points without an assigned value should be set equal to zero.)

(2) Geometry, General Control, and Film Geometry Card

Item Number (29 items, see fig. 11)

- 1 - M, number of mesh points in X-direction (13 points max)
- 2 - N, number of mesh points in Y-direction (30 points max)
- 3 - PLAMX = $6\mu U_b / P_a h_m^2$, bearing number in X-direction
- 4 - PLAMY = $6\mu V_b / P_a h_m^2$, bearing number in Y-direction

- 5 - YOX, circumferential length (Y-direction)/radial width (X-direction) for a single pad
- 6 - IH, number of points to first step in X-direction for first pad
- 7 - JH, number of points to first step in Y-direction for first pad
- 8 - IHH, number of points to second step in X-direction for first pad
- 9 - JHH, number of points to second step in Y-direction for first pad
- 10 - STEDE, ratio of step depth to film thickness for first pad
- 11 - NDIG, number of digits required for accuracy, usually for single pad set
- 12 - PFIX (1), dimensionless pressure, $P_1/P_1 = 1$
- 13 - PFIX (2), dimensionless pressure, P_2/P_1
- 14 - PFIX (3), dimensionless pressure, P_3/P_1
- 15 - NCASE, identify sets of input data
- 16 - LKOUNT, number of iterations allowed, usually set LKOUNT = 25
- 17 - IFLO = 2, for inlet flow in X-direction
- 18 - JFLO = 2, to N-1, for flow in Y-direction
- 19 - IFLOE = M-1, for outlet flow in X-direction
- 20 - COE (1) = C_1/L
- 21 - COE (2) = C_2/L
- 22 - COE (3) = 1
- 23 - COE (4) = C_4/C_3
- 24 - COE (5) = C_5/C_3
- 25 - COE (6) = C_6/C_3
- 26 - COE (7) = C_7/C_3
- 27 - COE (8) = C_8/C_3
- 28 - COE (9) = C_9/C_3
- 29 - COE (10) = C_{10}/C_3

The film thickness can be expressed in the third-degree polynomial as

$$h = C_3 + C_4(X-C_1) + C_5(Y-C_2) + C_6(X-C_1)^2 + C_7(Y-C_2)^2 + C_8(X-C_1)(Y-C_2) + C_9(X-C_1)^3 + C_{10}(Y-C_2)^3$$

For parallel film study, COE (3) = 1.0, and the rest of the coefficients are equal to zero. As for the detail for pivoting and tilting of the seal pad, reference 5 should be consulted.

(3) Final Control Card

Item Number (4 items)

- 1 - QUEP1 = T, print out P^2 after each iteration
F, omit P^2

- 2 - PPOUT1 = T, print out final P^2 after convergence
F, omit final P^2
- 3 - POUT1 = T, print out final pressure distribution
F, omit final pressure distribution
- 4 - NUKUE1 = T, read complete set of seal geometry cards, usually used
for first set

(4) Seal Geometry Cards

This set of data cards contains code numbers that describe each of the $M \times N$ nodal points. Each nodal point is designated as KUE in the computer program language. Since a two-dimensional array is stored columnwise in the computing machine, the MXN code numbers must be entered in columnwise order.

- KUE = 0, regular point or corner of depressed area
- KUE = 1, 2, or 3, corresponding to given pressure PFIX (1, 2, or 3)
- KUE = 4, vertical line of step in X-direction
- KUE = 5, horizontal line of step in Y-direction
- KUE = 6, TOP JOINT, leading edge in X-direction
- KUE = 7, BOTTOM JOINT, trailing edge in X-direction
- KUE = 8, LEFT JOINT, leading edge in Y-direction
- KUE = 9, RIGHT JOINT, trailing edge in Y-direction

Note that the joint condition implies that the boundary specified satisfies the cyclic boundary requirements. At present, the computer program is set up to handle correctly the cyclic boundary condition in the Y-direction. For this boundary condition, the mesh points in the Y-direction are increased from N to $N + 1$, and $N - 1$ divisions to N divisions for the total length of the seal pad. Furthermore, the input of N for cyclic boundary conditions should be equal to N , not $N + 1$, because the computer program increases the mesh points N to $N + 1$ automatically. The calculations for flow rate in the Y-direction for cyclic boundary conditions should set $JFLO = N$.

Comments on Use of Shrouded Rayleigh-Step Computer Program

The following remarks should be useful to a potential user of this program. Some of the limitations are stated.

(1) The number of mesh points is limited to 30 points in the Y-direction and 13 points maximum in the X-direction because of the 32K core storage capacity of the Lewis Research Center computer. Thus, a difficulty arises in checking to see if there is solution convergence of a particular geometric configuration and operating condition.

(2) The convergence of the numerical analysis is limited to moderate compressibility numbers. This difficulty may be overcome by incorporating the Newton-Raphson procedure. It is believed that convergence at higher compressibility numbers will be possible.

(3) An error occurs in the analysis in the step region where large gradients occur. This may explain the behavior shown in figure 6, where an optimum pocket length-to-land length ratio is not found.

Program Listing

```

$ISFTC TRIPAD LIST,DECK
C RINC10 REVISED BY DR.CHAS.NG 7,11,67 FOR MULTIPLE DEPRESSED FEED AND
C CORRECTED THE INTEGRATION FOR CYCLIC BOUNDARY CONDITION IN Y DIRECTION
C PROGRAM TO SOLVE STEP COMPRESS. BEAR. PROB. WITH FIXED
C BOUNDARIES, LINES OF SYMMETRY, JOINTS IN ANY DIRECTION.
C EQUATIONS ARE WRITTEN FOR PARALLEL FACES ONLY
C M , N ARE THE MESH POINTS IN THE X AND Y DIRECTIONS
C KUE=0 REGULAR POINT OR CORNER OF DEPRESSED AREA OR LINE OF SUMM
C KUE=1,2,3 KNOWN PRESSURE= PFIX(1,2,OR 3)
C KUE=4 VERTICAL LINE OF STEP
C KUE=5 HORIZONTAL LINE OF STEP
C KUE=6 TOP JOINT
C KUE=7 BOTTOM JOINT
C KUE=8 LEFT JOINT
C KUE=9 RIGHT JOINT
C PROBLEM IS SOLVED COLUMNWISE. M (FIRST INDEX)
C SHOULD BE SMALLER THAN N(SECOND INDEX)
C X IN I DIRECTION (VERT. DOWN)
C Y IN J DIRECTION (HOR. LEFT TO RIGHT)
C PLAMX,PLAMY=X,Y, COMPONENTS OF PLAM
C (IH,JH),(IHH,JHH) ARE CORNERS OF STOP BOUNDARY
C STEDF=STEP DEPTH. WHERE NO STEP H=1
C (IB,JB),(IBB,JBB) ARE CORNERS FOR SECOND PAD OR POCKET
C STEDR,STEP DEPTH FOR 2 PAD OR POCKET
C (IA,JA),(IAA,JAA) ARE CORNERS FOR SECOND OR THIRD PAD AND POCKET
C STEDA,STEP DEPTH FOR 2 OR 3 PAD AND POCKET
C NDIG= NO OF DIGITS WANTED REPEATED TO TRUNCATE SOLUTION
C LKOUNT IS THE MAXIMUM ALLOWABLE NUMBER OF ITERATIONS
C IFLO= I CCORDINATE OF THE LINE ACROSS WHICH Y-FLOW IS COMPUTED.
C JFLO= J CCORDINATE OF THE LINE ACROSS WHICH X-FLOW IS COMPUTED.
C COE= CLEARANCE COEFFICIENTS. SEE HFUN, HXFUN, HYFUN.
C QREP=.TRUE. PUT OUT P2 AFTEREACH ITERATION
C PPOUT=.TRUE. OUTPUT OF P2 AFTER CONVERGENCE
C POUT=.TRUE. WANTED OUTPUT OF P. AFTER CONVERGENCE
C NEWKUE=.TRUE. IF NEW KUE ARRAY IS READ IN
C TWO PAD SET NPD=TRUE AND THREE PAD SET NPD=FALSE
C NPAD=NO.OF PADS,SINGLE PAD=1,TWO PAD=2,THREE PAD=3
C NDPP=0 W/A/DP PRINTOUT, USE ONLY WHEN P2 IS GREATER THAN P1
C NDPP=1 USE ONLY FOR REGULAR GAS BEARING STUDIES
COMMON E,R,D
DIMENSION PFIX(3),KUE(13,30),QFIX(3),H(13,30),
IQ(13,30),FF(13,30),F(13),A(13,13),B(13),C(61),E(13,13,30),
IQSMA(13,13),G(13,30),R(13,13,30),S(13,30),PP(61),PX(61),
IPY(61),D(13,13,30),CQQ(61),COE(10)
I,XX(13),YY(61),PFX(13,30),PFY(13,30),HFX(13,30),HFY(13,30),F5(13,
130)
DIMENSION LOGCON(4),LOGKN1(4)
DATA LOGTRU/1HT/

```

```

EQUIVALENCE (LOGCON(1),QREP),(LOGCON(2),PPOUT),(LOGCON(3),POUT),
A      (LOGCON(4),NEWKUE),(LOGKNI(1),QREP1),(LOGKNI(2),PPOUT1),
B      (LOGKNI(3),POUT1),(LOGKNI(4),NUKUE1)
LOGICAL JOINT, QREP,PPOUT,PCUT,NEWKUE,NPD
LOGICAL LCGCON
NAMelist /CARD1/NPAD,INP,NDPP
NAMelist /CARD1A/IA,JA,IAA,JAA,STEDA,NPD
NAMelist /CARD1B/IB,JB,IBB,JBB,STEDB
NAMelist /CARD2/M,N,PLAMX,PLAMY,YOX,IH,JH,IHH,JHH,STEDE,NDIG,PFIX,
A NCASE,LKOUNT,IFLO,JFLO,IFLOE,COE
NAMelist /CARD3/QREP1,PPOUT1,POUT1,NUKUE1
NAMelist /CARD4/KUE
1 FORMAT(1X70I1)
3 FORMAT( 25H MATRIX IS SINGULAR AT J= I3,16H,CASE ABANDONED./1H1)
4 FORMAT( /          10(1X,F11.7))
5 FORMAT( //18H CASE CONVERGES TO I3,14H DIGITS AFTER I3,11H ITERATI
IONS)
6 FORMAT(//23H FINAL RESULTS FOR CASE I5//13H FORCE/AREA =E14.7,
1          64HCOEF OF CENTER OF PRESSURE IN PERCENTAGE OF SIDE
2DIMENSIONS = (E14.7,1H, E14.7,2H).)
7 FORMAT(46HOFLOW PER UNIT LENGTH IN X AT ENT. AND EXII = (
11PE14.7,2H, 1PE14.7,1H)24HFLOW PER U. L. IN Y = ( 1PE14.7,1H)//)
8 FORMAT(29H1FINAL PRESSURE DISTRIBUTION. //)
9 FORMAT(25H1FINAL P**2 DISTRIBUTION. /)
902 FORMAT(1H0,3HIA=,I5,3HJA=,I5,4HIAA=,I5,4HJAA=,I5,6HSTEDA=,E15.8)
903 FORMAT(1HC,3HIB=,I5,3HJB=,I5,4HIBB=,I5,4HJBB=,I5,6HSTEDB=,E15.8)
905 FORMAT(//23H FINAL RESULTS FOR CASE I5//13H FORCE/AREA =F14.7,7HW/
1A/DP=,E14.7/65H COEF OF CENTER OF PRESSURE IN PERCENTAGE OF SICE
2DIMENSIONS = (E14.7,1H, E14.7,2H).)
12 READ (5,CARD1)
GO TO (10,707,701) ,NPAD
701 READ(5,CARD1A)
IF (NPD) GO TO 10
707 READ(5,CARD1B)
10 READ (5,CARD2)
READ (5,CARD3)
WRITE (6,1002) QREP1,PPOUT1,POUT1,NUKUE1
1002 FORMAT (32H1 QREP PPOUT POUT NEWKUE/6XA1,6XA1,8XA1,6XA1)
DO 1004 MM=1,4
IF (LOGKNI(MM) .EQ. LOGTRU) GO TO 1006
LOGCON(MM) = .FALSE.
GO TO 1004
1006 LOGCON(MM) = .TRUE.
1004 CONTINUE
WRITE (6,1003) M,N, PLAMX, PLAMY, YOX, IH, JH, IHH, JHH, STEDE,
2          NDIG, PFIX, NCASE, LKOUNT, IFLO, JFLO, IFLOE, COE
1003 FORMAT(1H0,6X,1HM,5X,3HN ,21HPLAMX PLAMY YOX,7X,2HIH,6X,2HJH
2 5X,3HIHH 5X, 3HJHH/1H I7,I6,3F8.3,4I8/80H0 STEDE NDIG PFIX(1)
3 PFIX(2) PFIX(3) NCASE LKOUNT IFLO JFLO IFLOE/1H F7.3,I
45,F10.3,2F8.3,I7,2I8,I9,I7/6HOCOE = 10F8.3)
GO TO (702,703,704) ,NPAD
704 WRITE (6,902) IA,JA,IAA,JAA,STEDA
IF(NPD) GO TO 702
703 WRITE (6,903) IB,JB,IBB,JBB,STEDB
702 IF(.NOT.NEWKUE)GO TO 35
20 READ (5,CARD4)
DO 30 I=1,M
WRITE(6,1)(KUE(I,J),J=1,N)
DO 30 J=1,N

```

```

30 KUE(I,J)=KUE(I,J)+1
35 KOUNT=0
   NN=N-1
   MM=M-1
   DO 40 K=1,3
40 QFIX(K)= PFIX(K)*PFIX(K)
   DX=1./FLOAT(MM)
   IF(KUE(2,1).EQ.9.AND.PLAMY.GT.PLAMX) GO TO 44
   DY=YOX/FLCAT(NN)
   GO TO 43
44 DY=YOX/FLCAT(N)
43 DO 41 I=1,M
41 XX(I)=FLOAT(I-1)*DX
   DO 42 J=1, N
42 YY(J)=FLOAT(J-1)*DY
   SAA=1./DX
   SBB=1./DY
   SAA= SAA*SAA
   SBB=SBB*SBB
   SC=SAA+SBB
   SD=-2.*SC
   SE=PLAMX/(2.*DX)
   SEE=1./(2.*DX)
   SG=PLAMY/(2.*DY)
   SGG=1./(2.*DY)
   SH= 2.*SAA
   SI=2.*SBB
   SJ= 2.*SAA
   SK=2.*SBB
   DO 50 I=1,M
   DO 50 J=1,N
50 H(I,J)=HFUN(XX(I),YY(J),COE)
   GO TO (51,52,53) ,NPAD
53 DO 61 I=IA,IAA
   DO 61 J=JA,JAA
61 H(I,J)=H(I,J)+STEDA
   IF (NPD) GO TO 51
52 DO 62 I=IB,IBB
   DO 62 J=JB,JBB
62 H(I,J)=H(I,J)+STEDB
51 DO 60 I=IH,IHH
   DO 60 J=JH,JHH
60 H(I,J)=H(I,J)+STEDE
   DO 70 I=1,M
   DO 70 J=1,N
   Q(I,J)= 1
   HFX(I,J) =3.*HXFUN(XX(I),YY(J),COE)/H(I,J)
   HFY(I,J) =3.*HYFUN(XX(I),YY(J),COE)/H(I,J)
   ZZZ=-1.0/(H(I,J)*H(I,J))
   F5(I,J)=(2./3.)*ZZZ*(HFX(I,J)*PLAMX+HFY(I,J)*PLAMY)
   PFX(I,J)=PLAMX*ZZZ
70 PFY(I,J)=PLAMY*ZZZ
   JOINT=.FALSE.
80 DO 90 I=2,MM
   IF(KUE(I,1).EQ.9.OR.KUE(I,1).EQ.10) JOINT=.TRUE.
90 CONTINUE
100 DO 130 I=1,M
   G(I,1)=0.
   DO 110 K=1,M

```

```

110 E(I,K,1)=0.
    IF(.NOT.JCINT) GO TO 130
    DO 120 K=1,M
    D(I,K,1)=0.
    IF( I.EQ.K)D(I,K,1)=1.0
120 CONTINUE
130 CONTINUE
    DO 370 J=1,N
    DO 310 I=1,M
    FF(I,J)=1.0/SQRT(ABS(Q(I,J)))
    F(I)=0.
    KU= KUE (I,J)
    GO TO(140,210,210,210,230,250,270,270,140,140),KU
140 SGGG=SGG *(FF(I,J)*PFY(I,J)+HFY(I,J))
    C(I)=SBB+SGGG
    B(I)=SBB-SGGG
    DO 150 K=1,M
    A(I,K)=0.0
    IF(K.EQ.I)A(I,K)=SD+F5(I,J)*FF(I,J)
150 CONTINUE
    IF(JOINT) GO TO 180
    IF(J.NE.1) GO TO 160
    B(I)=0.
    C(I)=SK
160 IF (J.NE.N) GO TO 170
    C(I)=0.
    B(I)=SK
170 IF(I.EQ.1) GO TO 190
    IF(I.EQ.M) GO TO 200
180 SR=SEE*(FF(I,J)*PFX(I,J)+HFX(I,J))
    A(I,I+1)=SAA+SR
    A(I,I-1)=SAA-SR
    GO TO 310
190 A(I,I+1)=SJ
    GO TO 310
200 A(I,I-1)=SJ
    GO TO 310
210 K KU=KUE(I,J)-1
    B(I)=0.
    C(I)=0.
    F(I)=QFIX(KKU)
    DO 220 K=1,M
    A(I,K)=0.
    IF(I.EQ.K) A(I,K)=1.0
220 CONTINUE
    GO TO 310
230 HPLUS=H(I,J)
    HMINUS=H(I,J)
    GO TO (231,232,233),NPAD
233 IF (J.EQ.JA) HMINUS=HMINUS-STEDA
    IF (J.EQ.JAA) HPLUS=HPLUS-STEDA
    IF (NPD) GO TO 231
232 IF (J.EQ.JB) HMINUS=HMINUS-STEDB
    IF (J.EQ.JBB) HPLUS=HPLUS-STEDB
231 IF (J.EQ.JH) HMINUS=HMINUS-STEDE
    IF (J.EQ.JHH) HPLUS=HPLUS-STEDE
    HHH=HPLUS**3
    HH=HMINUS**3
    S8=.5*SB

```

```

      B(I)= -S8 * HH
      C(I)= -S8 * HHH
      DO 240 K=1,M
240  A(I,K)= 0.
      A(I,I)=S8*(HH+HHH)+PLAMY*( HPLUS-HMINUS)*FF(I,J)
      GO TO 310
250  HPLUS=H(I,J)
      HMINUS=H(I,J)
      IF ((IH .EQ. IB) .OR. (IH .EQ. IA)) GO TO 251
      GO TO (251,252,253),NPAD
253  IF(I.EQ. IA) HMINUS=HMINUS-STEDA
      IF (I.EQ. IAA) HPLUS=HPLUS-STEDA
      IF (NPD) GO TO 251
252  IF(I.EQ. IB) HMINUS=HMINUS-STEDB
      IF (I.EQ. IBB) HPLUS=HPLUS-STEDB
251  IF(I.EQ. IH) HMINUS=HMINUS-STEDE
      IF (I.EQ. IHH) HPLUS=HPLUS-STEDE
      HH=HMINUS**3
      HHH=HPLUS**3
      B(I)=0.
      C(I)=0.
      D9=2.*DX
      DO 260 K=1,M
260  A(I,K)=0.0
      A(I,I)=(HF+HHH)/D9-PLAMX*(HMINUS-HPLUS)*FF(I,J)
      A(I,I+1)=-HHH/D9
      A(I,I-1)=-HH/D9
      GO TO 310
270  SGGG=SGG*(FF(I,J)*PFY(I,J)+HFY(I,J))
      B(I)=SBB-SGGG
      C(I)=SBB+SGGG
      DO 280 K=1,M
      A(I,K)=0.0
      IF(K.EQ.I) A(I,K)=SD +F5(I,J)*FF(I,J)
280  CONTINUE
      SR=SEE*(FF(I,J)*PFX(I,J)+HFY(I,J))
      IF( KU. EQ.8) GO TO 290
      IF( KU.EQ.7) GO TO 300
      GO TO 310
290  A(I,1)=SAA+SR
      A(I,I-1)=SAA-SR
      GO TO 310
300  A(I,M)=SAA-SR
      A(I,I+1)=SAA+SR
      GO TO 310
310  CONTINUE
      DO 320 I=1,M
      DO 320 K=1,M
320  QSMA(I,K)=A(I,K) + B(I)*E(I,K,J)
      CALL MATINV(QSMA,M,BB,0,DET,ID)
      GO TO (340,330),ID
340  DO 360 I=1,M
      G(I,J+1)=0.
      DO 360 K=1,M
      G(I,J+1)=G(I,J+1)+QSMA(I,K)*(F(K)-B(K)*G(K,J))
      E(I,K,J+1)=-QSMA(I,K)*C(K)
      IF(.NOT.JCINT) GO TO 360
      DUM=0.0
      DO 350 KK=1,M

```

```

350 DUM=DUM-QSMA(I, KK)*B(KK)*D(KK, K, J)
    D(I, K, J+1)=DUM
360 CONTINUE
370 CONTINUE
    DMA=0.0
    IF(JOINT) GO TO 410
    DO 380 I=1, M
    DMA=AMAX1(DMA, ABS(Q(I, N)-G(I, N+1)))
380 Q(I, N)=G(I, N+1)
    DO 400 JJ=2, N
    J=N+2-JJ
    DO 400 I=1, M
    DUM=0.0
    DO 390 K=1, M
390 DUM=DUM+E(I, K, J)*Q(K, J)
    DUM=DUM+G(I, J)
    DMA=AMAX1(DMA, ABS(DUM-Q(I, J-1)))
400 Q(I, J-1)=DUM
    GO TO 560
410 DO 420 I=1, M
    DO 420 K=1, M
    QSMA(I, K)=-D(I, K, N+1)
    IF(I.EQ.K)QSMA(I, K)=QSMA(I, K)+1.0
420 CONTINUE
    CALL MATINV(QSMA, M, BB, 0, DET, ID)
    GO TO (430, 330), ID
330 WRITE(6, 3) J
    GO TO 12
430 DO 460 I=1, M
    DU=0.0
    DO 450 K=1, M
    DUM=0.0
    DO 440 KK=1, M
440 DUM=DUM+QSMA(I, KK)*E(KK, K, N+1)
    R(I, K, N)=DUM
450 DU=DU+QSMA(I, K)*G(K, N+1)
460 S(I, N)=DU
    DO 490 JJ=2, N
    J=N+2-JJ
    DO 490 I=1, M
    DU=0.0
    DO 480 K=1, M
    DUM=0.0
    DO 470 KK=1, M
470 DUM=D(I, KK, J)*R(KK, K, N)+E(I, KK, J)*R(KK, K, J)+DUM
    R(I, K, J-1)=DUM
480 DU=DU+D(I, K, J)*S(K, N)+E(I, K, J)*S(K, J)
490 S(I, J-1)=DU+G(I, J)
    DMA=0.0
    DO 500 I=1, M
    DO 500 K=1, M
    QSMA(I, K)=-R(I, K, 1)
    IF(I.EQ.K)QSMA(I, K)=QSMA(I, K)+1.0
500 CONTINUE
    CALL MATINV(QSMA, M, BB, 0, DET, ID)
    GO TO (510, 330), ID
510 DO 530 I=1, M
    DU=0.0
    DO 520 K=1, M

```

```

520 DU=DU+QSMA(I,K)*S(K,I)
    DMA=AMAX1(DMA,ABS(DU-Q(I,1)))
530 Q(I,1)=DU
    DO 550 J=2,N
    DO 550 I=1,M
    DU=0.0
    DO 540 K=1,M
540 DU=DU+R(I,K,J)*Q(K,I)
    DU=DU+S(I,J)
    DMA=AMAX1(DMA,ABS(DU-Q(I,J)))
550 Q(I,J)=DU
560 IF(QREP) WRITE(6,4)Q
    KOUNT=KOUNT+1
    IF(KOUNT.GE.LKOUNT)GO TO 561
    IF(DMA .GT. 10.0**FLOAT(-NDIG))GO TO 100
561 WRITE(6,5)NDIG,KOUNT
    IF(PPOUT)WRITE(6,9)
    DO 575 I=1,M
    IF(PPOUT)WRITE(6,4)(Q(I,J),J=1,N)
    DO 570 J=1,N
570 Q(I,J)=SQRT(ABS(Q(I,J)))
575 CONTINUE
    IF(POUT)WRITE(6,8)
    IF(KUE(2,1).EQ.9.AND.PLAMY.GT.PLAMX) GO TO 571
    DO 576 I=1,M
    IF(POUT)WRITE(6,4)(Q(I,J),J=1,N)
576 CONTINUE
    GO TO 573
571 NE=N+1
    DO 572 I=1,M
    H(I,NE)=H(I,1)
    Q(I,NE)=Q(I,1)
    IF(POUT) WRITE(6,4) (Q(I,J),J=1,NE)
572 CONTINUE
573 IF(KUE(2,1).EQ.9.AND.PLAMY.GT.PLAMX) GO TO 700
    DO 590 I=1,M
    X= DX*FLOAT(I-1)
    DO 580 J=1,N
580 QQQ(J)=Q(I,J)-1.0
    PP(I)= SUM(CQQ,N,DY)
590 PX(I)= PP(I)*X
    DO 610 J=1,N
    Y= FLOAT(J-1)*DY
    DO 600 I=1,M
600 QQQ(I)=Q(I,J)-1.0
610 PY(J)=SUM(CQQ,M,DX)*Y
    FP= SUM(PP,M,DX)
    FX= SUM(PX,M,DX)
    XF =FX/FP
    FY= SUM(PY,N,DY)
    GO TO 745
700 DO 710 I=1,M
    X=DX*FLOAT(I-1)
    DO 720 J=1,NE
720 QQQ(J)=Q(I,J)-1.0
    PP(I)=SUM(CQQ,NE,DY)
710 PX(I)=PP(I)*X
    DO 730 J=1,NE
    Y=FLOAT(J-1)*DY
    DO 740 I=1,M

```

```

740 QQQ(I)=Q(I,J)-1.
730 PY(J)=SUM(QQQ,M,DX)*Y
    FP=SUM(PP,M,DX)
    FX=SUM(PX,M,DX)
    XF = FX/FP
    FY=SUM (PY,NE,DY)
745 YF=FY/FP/YOX
    FP=FP/YOX
    IF(NDPP) 880,880,881
880 FDP=FP/(PFIX(2)-PFIX(1))
    WRITE (6,905) NCASE,FP,FDP,XF,YF
    GO TO 882
881 WRITE(6,6) NCASE,FP,XF,YF
882 DO 620 I=1,M
620 PP(I)=Q(I,JFLO)*H(I,JFLO)*(-PLAMY+H(I,JFLO)**2
    1*(Q(I,JFLC+1)-Q(I,JFLO-1)))/(2.*DY))
    FLOY=SUM(PP,M,DX)
    NFLO=1
    IFLT=IFLO
625 IF(KUE(2,1).EQ.9.AND.PLAMY.GT.PLAMX) GO TO 750
    DO 630 J=1,N
630 PP(J)=Q(IFLT,J)*H(IFLT,J)*(-PLAMX+H(IFLT,J)**2
    1*(Q(IFLT+1,J)-Q(IFLT-1,J)))/(2.*DX))
    FLOT=SUM(PP,N,DY)/YOX
    GO TO 770
750 DO 760 J=1,NE
760 PP(J)=Q(IFLT,J)*H(IFLT,J)*(-PLAMX+H(IFLT,J)**2
    1*(Q(IFLT+1,J)-Q(IFLT-1,J)))/(2.*DX))
    FLOT=SUM (PP,NE,DY)/YOX
770 GO TO (635,636),NFLO
635 NFLO=2
    FLOX=FLOT
    IFLT=IFLOE
    GO TO 625
636 CONTINUE
    WRITE(6,7) FLOT,FLOX,FLOY
    IF(INP) 12,12,800
800 STOP
    END

```

```

$IBFTC SUM      LIST,DECK
    FUNCTION SUM(P,M,DX)
    DIMENSION P(70)
    IF((M/2)*2-M) 80;81,81
80 K=2
    KK=M-1
    KKK=?
    SUM=0.0
10 DO 20 I=K,KK,KKK

```

```

20 SUM=SUM+P(I)
   GO TO (30,40,50),K
30 SUM=SUM*DX/3.0
   RETURN
40 K=3
45 SUM=2.0*SUM
   GO TO 10
50 K=1
   KK=M
   KKK=M-1
   GO TO 45
81 SUM=P(1)-P(M)
   SUM=SUM +.25*P(1)+3.*P(2)-.25*P(3)
   DO 60 J=3,M,2
   SUM = SUM +4.*P(J)+2.*P(J+1)
60 CONTINUE
   SUM = SUM *DX/3.
   RETURN
   END

```

```

$IBFTC HFUN    LIST,DECK
      FUNCTION HFUN (XX,YY,COE)
C      FUNCTION TO EVALUATE CLEARANCE H FROM X,Y AND COEFFICIENTS COE
      DIMENSION COE(10)
      X=XX-COE(1)
      Y=YY-COE(2)
      HFUN=COE(3)+COE(4)*X+COE(5)*Y+COE(6)*X*X+
1COE(7)*Y*Y+COE(8)*X*Y+COE(9)*X*X*X+
2COE(10)*Y*Y*Y
      RETURN
      END

```

```

$IBFTC HXFUN    LIST,DECK
      FUNCTION HXFUN(XX,YY,COE)
C      FUNCTION TO EVALUATE X-DERIVATIVE OF H FROM X,Y AND COEFFICIENTS C
      DIMENSION COE(10)
      X=XX-COE(1)
      Y=YY-COE(2)
      HXFUN=COE(4)+2.*COE(6)*X+COE(8)*Y+
13.*COE(9)*X*X
      RETURN
      END

```

```

$IBFTC HYFUN LIST,DECK
FUNCTION HYFUN(XX,YY,COE)
C FUNCTION TO EVALUATE Y-DERIVATIVE OF H FROM X,Y AND COEFFICIENTS C
DIMENSION COE(10)
X=XX-COE(1)
Y=YY-COE(2)
HYFUN=COE(5)+2.*COE(7)*Y+COE(8)*X+3.*COE(10)*Y*Y
RETURN
END

```

```

$IBFTC MATINV LIST,DECK
C MATRIX INVERSION WITH ACCOMPANYING SOLUTION OF LINEAR EQUATIONS
C NOVEMBER 1962 S GOOD DAVID TAYLOR MODEL BASIN AM MAT1
SUBROUTINE MATINV(A,N1,B,M1,DETERM,ID)
C GENERAL FORM OF DIMENSION STATEMENT
DIMENSION A(13,13),B(13,1),INDEX(13,3)
EQUIVALENCE (IROW,JROW), (ICOLM,JCOLUM), (AMAX, T, SWAP)
M=M1
N=N1
10 DETERM=0.0
15 DO 20 J=1,N
20 INDEX(J,3) = 0
30 DO 550 I=1,N
C SEARCH FOR PIVOT ELEMENT
40 AMAX=0.0
45 DO 105 J=1,N
IF(INDEX(J,3)-1) 60, 105, 60
60 DO 100 K=1,N
IF(INDEX(K,3)-1) 80, 100, 715
80 IF ( AMAX -ABS (A(J,K))) 85, 100, 100
85 IROW=J
90 ICOLUM=K
AMAX = ABS (A(J,K))
100 CONTINUE
105 CONTINUE
INDEX(ICOLUM,3) = INDEX(ICOLUM,3) +1
260 INDEX(I,1)=IROW
270 INDEX(I,2)=ICOLUM
C INTERCHANGE ROWS TO PUT PIVCT ELEMENT ON DIAGONAL
130 IF (IROW-ICOLUM) 140, 310, 140
140 DETERM=-DETERM
150 DO 200 L=1,N
160 SWAP=A(IROW,L)
170 A(IROW,L)=A(ICOLUM,L)
200 A(ICOLUM,L)=SWAP
IF(M) 310, 310, 210
210 DO 250 L=1,M
220 SWAP=B(IROW,L)
230 B(IROW,L)=B(ICOLUM,L)
250 B(ICOLUM,L)=SWAP

```

```

C      DIVIDE PIVOT ROW BY PIVOT ELEMENT
310 PIVOT  =A(ICOLUM,ICOLUM)
      DETERM=DETERM*PIVOT
330 A(ICOLUM,ICOLUM)=1.0
340 DO 350 L=1,N
350 A(ICOLUM,L)=A(ICOLUM,L)/PIVOT
355 IF(M) 380, 380, 360
360 DO 370 L=1,M
370 B(ICOLUM,L)=B(ICOLUM,L)/PIVOT
C      REDUCE NON-PIVOT ROWS
380 DO 550 L1=1,N
390 IF(L1-ICOLUM) 400, 550, 400
400 T=A(L1,ICOLUM)
420 A(L1,ICOLUM)=0.0
430 DO 450 L=1,N
450 A(L1,L)=A(L1,L)-A(ICOLUM,L)*T
455 IF(M) 550, 550, 460
460 DO 500 L=1,M
500 B(L1,L)=B(L1,L)-B(ICOLUM,L)*T
550 CONTINUE
C      INTERCHANGE COLUMNS
600 DO 710 I=1,N
610 L=N+1-I
620 IF (INDEX(L,1)-INDEX(L,2)) 630, 710, 630
630 JROW=INDEX(L,1)
640 JCOLUM=INDEX(L,2)
650 DO 705 K=1,N
660 SWAP=A(K,JROW)
670 A(K,JROW)=A(K,JCOLUM)
700 A(K,JCOLUM)=SWAP
705 CONTINUE
710 CONTINUE
      DO 730 K =1,N
      IF(INDEX(K,3) -1) 715,720,715
720 CONTINUE
730 CONTINUE
      ID=1
      GO TO 740
715 ID =2
740 RETURN
      END

```

Sample Problem

An example of the use of the computer program is given for the 315 psia (217 N/cm²) design point for both a parallel film and a film with a 2-milliradian tilt. The geometry is shown in figures 4 and 11. The mean film thickness to be investigated h_m is 0.0003 inch (0.0008 cm), and the groove depth Δ is 0.0001 inch (0.0003 cm).

From table II for $h_m = 0.0003$ inch (0.0008 cm),

$$\Lambda_y = 1.715 = \text{PLAMY} \quad \text{PLAMX} = 0 = \Lambda_x$$

TABLE II. - SUMMARY OF COMPRESSIBILITY NUMBER FOR EACH
FILM THICKNESS AT EACH DESIGN POINT

Film thickness, h_m		Design point		
		1	2	3
in.	cm	Sealed pressure, P_1		
		65 psia (45 N/cm ² abs)	215 psia (148 N/cm ² abs)	315 psia (217 N/cm ² abs)
		Compressibility number, Λ_y		
0.0001	0.0003	15.2	20.4	15.4
.0002	.0005	3.80	5.10	3.86
.0003	.0008	1.69	2.27	1.715
.0004	.0010	.950	1.28	.965
.0005	.0013	.650	.816	.617
.0006	.0015	.423	.567	.428
.0007	.0018	.311	.417	.315
.0008	.0020	.238	.319	.241
.0009	.0023	.188	.252	.191
.0010	.0025	.152	.204	.154

$$YOX = \frac{c}{b} = \frac{0.878}{0.25} = 3.500$$

$$STEDE = \frac{\Delta + h_m}{h_m} = 3.3$$

$$PFIX(1) = \frac{P_1}{P_1} = 1$$

$$PFIX(2) = \frac{P_2}{P_1} = 1$$

For the parallel film case,

$$\bar{C}_1 = 0$$

$$\bar{C}_2 = 0$$

$$\bar{C}_3 = \text{Coe}(3) = 1$$

$$\bar{C}_4 = 0$$

For the 2-milliradian tilt case,

$$\bar{C}_1 = \text{Coe}(1) = \frac{C_1}{b} = \frac{0.5b}{b} = 0.5$$

$$\bar{C}_2 = 0$$

$$\bar{C}_3 = 1$$

$$\bar{C}_4 = \frac{\alpha b}{h_m} = \frac{(0.002)(0.25)}{0.0003} = 1.667$$

The data for this sample problem are shown in tables III and IV. The execution time for this problem was about 0.21 minute on the Lewis Research Center computer. (Note, however, that the execution time increases with Λ_y since the total number of iterations increases.) The sample output is as follows:

For the parallel film case,

$$\bar{W} = \frac{\text{force}}{\text{area}} = 0.03813818$$

$$\frac{\text{load}}{\text{pad}} = \frac{W}{\text{pad}} = \bar{W} P_a bc = \frac{2.517 \text{ lb}}{\text{pad}}$$

or

$$\frac{\text{load}}{\text{pad}} = \frac{W}{\text{pad}} = \bar{W} P_a bc = \frac{1.144 \text{ kg}}{\text{pad}}$$

The total load for 20 pads is 50.34 pounds (22.90 kg).

For the 2-milliradian tilt case,

$$\bar{W} = \frac{\text{force}}{\text{area}} = 0.03056596$$

$$W = \bar{W} P_a bc = \frac{2.0175 \text{ lb}}{\text{pad}}$$

or

$$W = \bar{W} P_a bc = \frac{0.915 \text{ kg}}{\text{pad}}$$

The total load is 40.35 pounds (21.85 kg).

A check was made to see if the solution was the correct converged solution by changing the mesh size, as shown with the following results:

M	N	Force/area
7	14	0.03863340
7	27	.03758219
13	14	.03973810
13	27	.03813818

Since the results agree satisfactorily, the solution is considered converged.

REFERENCES

1. Parks, A. J.; McKibbin, R. H.; and Ng, C. C. W.: Development of Main Shaft Seals for Advanced Air Breathing Propulsion Systems. Rep. PWA-3161, Pratt & Whitney Aircraft (NASA CR-72338), Aug. 14, 1967.
2. Shevchenko, Richard P.: Shaft, Bearing and Seal Systems For a Small Engine. Paper 670064, SAE, Jan. 1967.
3. McKibbin, A. H.; and Park, A. J.: Aircraft Gas Turbine Mainshaft Face Seals - Problems and Promises. Paper FICFS-28, ASLE, May 1969.
4. Hawkins, R. M.; McKibbin, A. H.; and Ng, C. C. W.: Development of Compressor Seals, Stator Interstage Seals, and Stator Pivot Seals in Advanced Air Breathing Propulsion Systems. Rep. PWA-3147, Pratt & Whitney Aircraft (NASA CR-95946), July 20, 1967.
5. Hawkins, R. M.: Development of Compressor End Seals, Stator Interstage Seals, and Stator Pivot Seals in Advanced Air Breathing Propulsion Systems. Rep. PWA-2875, Pratt & Whitney Aircraft (NASA CR-83786), July 20, 1966.
6. Cheng, H. S.; Castelli, V.; and Chow, C. Y.: Performance Characteristics of Spiral-Groove and Shrouded Rayleigh-Step Profiles for High-Speed Non-Contacting Gas Seals. J. Lubr. Tech., vol. 91, no. 1, Jan. 1969, pp. 60-68.
7. Hawkins, R. M.; and Knapp, C. A.: Development of Compressor End Seals, Stator Interstage Seals, and Stator Pivot Seals in Air Breathing Propulsion Systems. Rep. PWA-2752, Pratt & Whitney Aircraft (NASA CR-54625), Jan. 20, 1966.